MAJOR ARTICLE

Lethal Crimean-Congo Hemorrhagic Fever Virus Infection in Interferon α/β Receptor Knockout Mice Is Associated With High Viral Loads, Proinflammatory Responses, and Coagulopathy

Marko Zivcec,[1,3] David Safronetz,[1] Dana Scott,[2] Shelly Robertson,[1] Hideki Ebihara,[1] and Heinz Feldmann[1,3]

[1]Laboratory of Virology and [2]Rocky Mountain Veterinary Branch, Division of Intramural Research, National Institute Allergy and Infectious Disease, National Institutes of Health, Rocky Mountain Laboratories, Hamilton, Montana; and [3]Department of Medical Microbiology and Infectious Diseases, University of Manitoba, Winnipeg, Canada

Crimean-Congo hemorrhagic fever (CCHF) is a widely distributed viral hemorrhagic fever characterized by rapid onset of flu-like symptoms often followed by hemorrhagic manifestations. CCHF virus (CCHFV), a bunyavirus in the *Nairovirus* genus, is capable of infecting a wide range of mammalian hosts in nature but so far only causes disease in humans. Recently, immunocompromised mice have been reported as CCHF disease models, but detailed characterization is lacking. Here, we closely followed infection and disease progression in CCHFV-infected interferon α/β receptor knockout (IFNAR$^{-/-}$) mice and age-matched wild-type (WT) mice. WT mice quickly clear CCHFV without developing any disease signs. In contrast, CCHFV infected IFNAR$^{-/-}$ mice develop an acute fulminant disease with high viral loads leading to organ pathology (liver and lymphoid tissues), marked proinflammatory host responses, severe thrombocytopenia, coagulopathy, and death. Disease progression closely mimics hallmarks of human CCHF disease, making IFNAR$^{-/-}$ mice an excellent choice to assess medical countermeasures.

Keywords. CCHFV; interferon α/β receptor knockout mice; coagulopathy; thrombocytopenia; pathology; proinflammatory response.

Crimean-Congo hemorrhagic fever (CCHF) is the second most widely distributed viral hemorrhagic fever, with an area of endemicity spanning western, central, and southern Africa, the Balkans, the Middle East, southern Russia, and western Asia [1–3]. The etiologic agent is CCHF virus (CCHFV), a bunyavirus in the *Nairovirus* genus, which is thought to be primarily maintained in ticks of the *Hyalomma* genus of the *Ixodidae* family. In nature, CCHFV has a wide host range and causes a transient viremia in many wild, domesticated, and laboratory mammals [1–5], but infection is refractory in most birds [6, 7]. CCHFV is transmitted to humans via multiple routes, including by the bite of an infected tick, by crushing an engorged infected tick, or by contact with infected body fluids of viremic humans or animals [1–3].

CCHFV infection in humans is characterized by 4 distinct phases: incubation, prehemorrhagic, hemorrhagic, and convalescence. The incubation phase lasts 1–7 days after exposure, although incubation periods of >13 days have been documented [1–3, 8]. The prehemorrhagic phase spans 3–7 days and is characterized by rapid onset of fever (temperature >39.0°C), fatigue, cephalalgia, dizziness, photophobia, and myalgia, but it may also include nausea, vomiting, and diarrhea [1–3]. Severe cases of CCHF progress to the hemorrhagic phase, which lasts 2–3 days and is characterized by petechiae, ecchymosis, epistaxis, gingival

Received 22 June 2012; accepted 14 August 2012; electronically published 15 February 2013.

Correspondence: Heinz Feldmann, MD, RML, 903 S 4th St, Hamilton, MT 59840 (feldmannh@niaid.nih.gov).

The Journal of Infectious Diseases 2013;207:1909–21
Published by Oxford University Press on behalf of the Infectious Diseases Society of America 2013.
DOI: 10.1093/infdis/jit061

hemorrhage and often includes gastrointestinal and cerebral hemorrhage. It is during the hemorrhagic phase that patients die of CCHF, with the predictors of fatal outcome being high viral loads, increased serum aspartate and alanine aminotransferase levels, thrombocytopenia, increased clotting times, increased serum levels of proinflammatory cytokines and chemokines, low antibody titers, and presence of melena [9–19]. The main targets of virus infection in humans are mononuclear phagocytes, endothelial cells, and hepatocytes [20, 21]. Severe liver necrosis, shock, and subsequent multiorgan failure are the main causes of death [1–3, 20]. The case-fatality rate is approximately 30% [1–3], although it can vary among geographical locations, ranging from approximately 5% in a Turkish outbreak [22] to 60% in a United Arab Emirates outbreak [23]. Convalescence occurs 10–20 days after symptom onset and may include clinical symptoms such as tachycardia, polyneuritis, breathing impairment, poor vision, loss of hearing, and loss of memory [1–3]. Despite a wide distribution, the pathogenesis of CCHF remains poorly understood because of limited human pathology data and the need for high-containment facilities to handle CCHFV-infected specimens.

With the exception of humans, no immunocompetent mammal is known to develop signs of disease following CCHFV infection [1–3], which has significantly hampered the development of CCHF disease models for pathogenesis studies and efficacy testing of medical countermeasures. Suckling mice develop disease following CCHFV inoculation, but the disease has little similarity to human CCHF [24]. Recently, adult mice with gene knockouts of the signal transducer and activator of transcription 1 ($STAT1^{-/-}$) or the interferon α/β receptor ($IFNAR^{-/-}$) have been described as models of lethal CCHFV infection [25, 26]. Here, we evaluated the sensitivity of $IFNAR^{-/-}$ mice to several routes of exposure and conducted a time course analysis of the pathologic, virologic, hematologic, biochemical, and immunologic parameters associated with CCHFV infection. Our results show that the $IFNAR^{-/-}$ model recapitulates human CCHF by showing most of the clinical hallmarks, which makes it a suitable model to evaluate medicinal countermeasures against CCHFV infections.

METHODS

Ethics and Biosafety Statements

Animal experiments were approved by the institutional animal care and use committee and performed following the guidelines of the Association for Assessment and Accreditation of Laboratory Animal Care, International (AAALAC) by certified staff in an AAALAC-approved facility (A4149-01). All procedures involving infectious CCHFV were performed in a biosafety level 4 (BSL4) facility according to standard operating procedures approved by the institutional biosafety committee.

Animals, Virus Stocks and Viral Titration

IFNAR$^{-/-}$ C57BL/6 mice aged 6–12 weeks (breeding pairs kindly provided by Dr Genhong Cheng, University of California Los Angeles) were obtained from an in-house breeding colony. Age-matched wild-type (WT) C57BL/6 mice were purchased from Jackson Laboratories (Sacramento, CA). Prior to experiments, mice were acclimatized to BSL4 conditions in an enriched, sterile environment with access to food and water ad libitum. CCHFV strain IbAr 10200 (kindly provided by Dr Michael Holbrook, University of Texas Medical Branch, Galveston) was propagated in SW13 cells maintained in Leibovitz's L-15 medium (both from ATCC, Manassas, VA) supplemented with 10% heat-inactivated fetal bovine serum, 100 mM L-glutamine, and 50 U/mL penicillin, and 50 μg/mL streptomycin (Sigma-Aldrich, St. Louis, MO) in an environment not enriched in CO_2. Viral titers were determined using standard methods (as outlined below) and expressed as 50% tissue culture infectious doses ($TCID_{50}$) per milliliter.

Assessing the Route of Inoculation

Groups of 6 $IFNAR^{-/-}$ mice were inoculated with 10^2 or 10^4 $TCID_{50}$ of virus diluted in L-15 medium, by the intraperitoneal route (100 μL total volume delivered by single injection into the bottom-left quadrant), the intramuscular route (100 μL total volume delivered by single injection into the hind-leg musculature), the intranasal route (50 μL total volume, 25 μL per nare), and the subcutaneous/intradermal route (50 μL total volume delivered by a single injection between the shoulders). Weights and health evaluations were performed daily for the first 10 days after infection, and surviving mice were monitored for signs of illness until 21 days after infection. To determine the 50% lethal dose (LD_{50}) of CCHFV in $IFNAR^{-/-}$ mice, CCHFV was diluted in L-15 medium in log_{10} increments (10^2–10^{-3} $TCID_{50}$) and inoculated into groups of 6 mice by the subcutaneous route, as described above. Mice were monitored daily for 21 days after infection.

Serial Sacrifice Study

Groups of 6 WT or $IFNAR^{-/-}$ mice were inoculated with 200 LD_{50} (representing a challenge dose of 10 $TCID_{50}$) of CCHFV by the subcutaneous route, as outlined above. At 12 hours, and daily between days 1 and 5 after infection, one group of $IFNAR^{-/-}$ and WT mice was exsanguinated by cardiac puncture, with whole blood collected into tubes containing ethylenediaminetetraacetic acid (EDTA; BD Biosciences, Sparks, MD) and frozen at −80°C for virus isolation or RNA extraction. Mice were necropsied, and lung, heart, liver, kidney, spleen, cervical lymph nodes, and brain specimens were collected and immediately frozen at −80°C for virus isolation. Because of the volume of blood required for hematologic analysis and monitoring coagulation parameters, a follow-up study was conducted with groups of 15 $IFNAR^{-/-}$ or WT mice

inoculated as above. On days 1–5 after infection, one group of IFNAR$^{-/-}$ and WT mice was exsanguinated, with whole blood collected in EDTA-loaded syringes (6 mice per time point, for hematologic analysis) or sodium citrate–loaded syringes (9 mice, for assessment of coagulation parameters; final citrate concentration, 0.0105 M).

Virus Titration

Virus titration was performed on 10-fold serial dilutions (prepared in L-15 media) of tissue (10% w/v solution) and blood (10% v/v solution) samples, using a standard $TCID_{50}$ assay on SW-13 cells in 96-well plates [27]. Plates were incubated for 6 days at 37°C without increased CO_2, and wells were scored for cytopathic effect. Virus concentrations were calculated using the Reed and Münch formula [28] and expressed as $TCID_{50}$ per milligram of tissue.

CCHFV-Specific Quantitative Reverse Transcription Polymerase Chain Reaction (RT-PCR) Analysis

CCHFV S segment specific primers (CCHFSFw–TGGACTTG TGGACACCTTCAC, CCHFSRe–CAATGCCAGTGGAGCTA ACC) and probe (CCHFSPr-6FAM–TGCCTCCACCAGAGC AGATGCGT–BBQ) were designed and synthesized by TIB MOLBIOL (Adelphia, NJ). RNA from whole blood was extracted using the NucleoSpin 96 Virus Core Kit (Macherey-Nagel, Bethlehem, PA) according to the manufacturer's instructions. Quantitative RT-PCR assays were performed on the Rotor-Gene 6000 thermocycler (Corbett, San Francisco, CA), using the QuantiFast Probe RT-PCR kit (Qiagen, Valencia, CA) according to the manufacturer's instructions. $TCID_{50}$ equivalents were calculated from a standard curve generated using $\log_{10}$ dilutions of RNA extracted from the CCHFV stock.

Histopathologic and Immunohistochemistry (IHC) Analysis

Tissue samples were fixed in 10% neutral-buffered formalin according to approved standard operating procedures. Following fixation, samples were processed with a Sakura VIP-5 Tissue Tek instrument (Torrance, CA), using a graded series of ethanol, xylene, and ParaPlast Extra (EMS, Hatfield, PA). Embedded tissues were sectioned at 5 μm and dried overnight at 42°C prior to being stained with hematoxylin and eosin. Phosphotungstic acid haematoxylin (PTAH) staining was accomplished using a P.T.A.H. stain kit (American MasterTech, Lodi, CA). IHC analysis was performed on a Discovery XT automated processor (Ventana Medical Systems, Tucson, AZ) using a custom rabbit sera (NP_{1028}) raised against a CCHFV nucleoprotein peptide (residues 10–28; Open Biosystems, Rockford, IL) as the primary anti-CCHFV antibody (1:100 dilution) and the DAPMap kit (Ventana Medical Systems). Slides were examined by a veterinary pathologist and scored as follows: 0, no obvious pathologic changes; 1, minimal increase in the number of inflammatory cells and hepatocellular necrosis; 2, mildly increased numbers of inflammatory degenerate cells, hepatocellular necrosis, or lymphocytolysis; 3, moderately increased numbers of inflammatory degenerate cells, and hepatocellular necrosis or lymphocytolysis; and 4, highly increased numbers of inflammatory degenerate cells and multifocal hepatocellular necrosis or lymphocytolysis.

Hematologic, Coagulation, and Blood Chemistry Parameters

Total white blood cell count, lymphocyte, platelet, reticulocyte and red blood cell counts, hemoglobin concentration, hematocrit values, mean cell volume, mean corpuscular volume, mean platelet volume, and mean corpuscular hemoglobin concentration were analyzed in EDTA-treated whole blood on a HemaVet 950FS1 laser-based hematology analyzer (Drew Scientific, Dallas, TX). Plasma from citrate-treated blood was tested for coagulation parameters, including prothrombin time, activated partial thromboplastin time, and fibrinogen concentration, using the PTT Automate, STA Neoplastine CI plus, and Fibri-Prest automate respectively, on a STart4 instrument (all from Diagnostica Stago, Parsippany, NJ) according to the manufacturer's instructions. Citrate-treated plasma samples were pooled (a pool of 6 plasma samples on days 1–4 after infection and a pool of 3 plasma samples on day 5 after infection) and tested for concentrations of albumin, amylase, alanine aminotransferase (ALT), aspartate aminotransferase (AST), alkaline phosphatase, γ-glutamyltransferase, glucose, cholesterol, total protein, total bilirubin, blood urea nitrogen, and creatinine by using a Piccolo point-of-care blood analyzer (Abaxis, Sunnyvale, CA).

Chemokine and Cytokine Analysis

Plasma levels of granulocyte colony stimulating factor (G-CSF), granulocyte-macrophage colony stimulating factor (GM-CSF), interferon γ (IFN-γ), interleukin 1α (IL–1α), interleukin 1β (IL-1β), interleukin 2 (IL-2), interleukin 4, interleukin 5, interleukin 6 (IL-6), interleukin 7, interleukin 9, interleukin 10 (IL-10), interleukin 12p70 (IL-12p70), interleukin 13 (IL-13), interleukin 15, interleukin 17 (IL-17), IFN-γ–induced protein 10 (CXCL10), chemokine (C-X-C motif) ligand 1 like (CXCL1), monocyte chemotactic protein 1 (CCL2), macrophage inflammatory protein 1α (CCL3), regulated upon activation, normal T-cell expressed and secreted (CCL5), and tumor necrosis factor α (TNF-α) were determined using the Milliplex MAP Mouse Cytokine/Chemokine kit (Millipore, Billerica, MA) according to the manufacturer's instructions. Samples were read on a Bio-Plex 200 system instrument (Bio-Rad, Hercules, CA).

Statistical Analysis

Coagulation and hematologic parameters and plasma cytokine/chemokine concentrations were compared with those of uninfected controls, using 1-way analysis of variance with the Dunnet posttest on GraphPad Prism v5.00 (GraphPad Software, La Jolla, CA).

RESULTS AND DISCUSSION

IFNAR$^{-/-}$ Mice Are Susceptible to CCHFV via Multiple Routes of Infection

IFNAR$^{-/-}$ mice are sensitive to numerous viral pathogens because of an inability to respond to type I IFN signaling. Therefore, CCHFV, an IFN-sensitive virus [29, 30], is thought to cause severe disease in IFNAR$^{-/-}$ mice through uncontrolled replication. A similar disease course is thought to occur in severe cases of human CCHF, as ineffective immune responses against CCHFV and/or effective host interferon antagonism allow the virus to replicate to high levels [11, 12, 31–34]. Human CCHF seems to differ in onset of symptoms and clinical outcome depending on the route of infection [2, 33]. To assess susceptibility to those routes of infection, IFNAR$^{-/-}$ mice were infected with 10^4 $TCID_{50}$ of CCHFV by the intraperitoneal, intranasal, intramuscular, and subcutaneous routes. The intraperitoneal route was chosen because it was used as a surrogate route for intravenous infection and previously resulted in fulminant disease in IFNAR$^{-/-}$ mice, while the intranasal, intramuscular, and subcutaneous routes of inoculation were chosen to mimic natural routes of human infection by droplets, percutaneous injury, and tick bite, respectively. All routes of infection resulted in rapid development of severe disease, which was ultimately fatal within 3–5 days (Figure 1*A*). Signs of infection were first apparent 2 days before death and included weight loss (Figure 1*A*), ruffled fur, hunched posture, and lethargy. A difference in disease onset

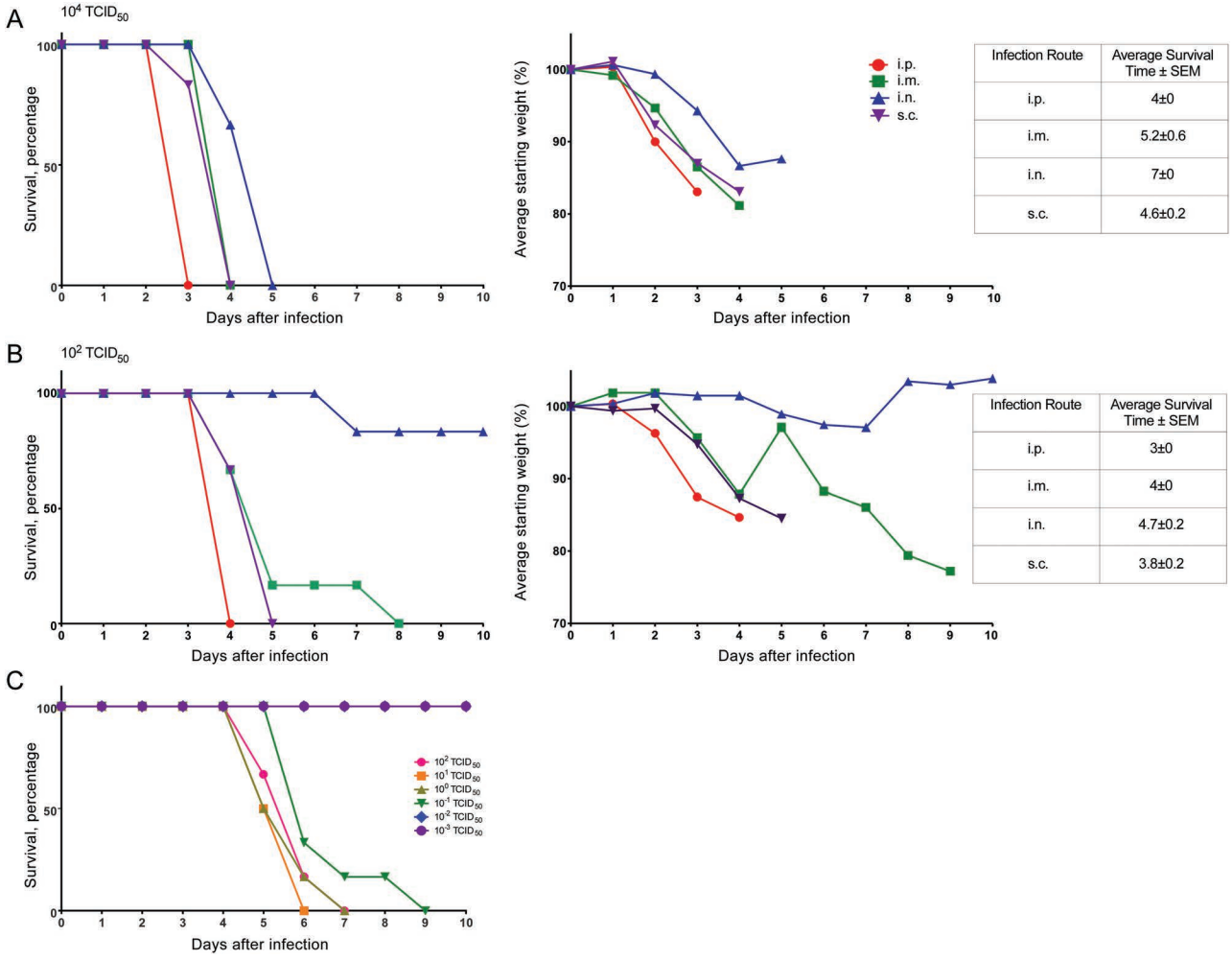

Figure 1. Survival and weight loss among IFNAR$^{-/-}$ mice following infection with Crimean-Congo hemorrhagic fever virus (CCHFV) by different routes. Groups of 6 IFNAR$^{-/-}$ mice were challenged with a high (10^4 median tissue culture infective doses [$TCID_{50}$]; *A*) and a low (10^2 $TCID_{50}$; *B*) dose of CCHFV by the intraperitoneal (i.p.), intramuscular (i.m.), intranasal (i.n.), and subcutaneous (s.c.) routes of inoculation. *A*, At the high dose of CCHFV, IFNAR$^{-/-}$ mice rapidly succumb to infection and display disease signs, including weight loss (right graph; note, IFNAR$^{-/-}$ mice were weighed daily as a group), ruffled fur, hunched posture, and lethargy. *B*, At the low dose of CCHFV, IFNAR$^{-/-}$ mice develop similar disease but exhibit a delayed onset and time to death. *C*, The IFNAR$^{-/-}$ mouse 50% lethal dose for the s.c. route was determined using the standard $TCID_{50}$ assay to be 0.05 $TCID_{50}$. Abbreviation: SEM, standard error of the mean.

following the different routes of inoculation was observed, with the intraperitoneal route demonstrating the most rapid onset of disease and the intranasal route demonstrating the slowest onset of disease. Similarly, inoculation with 10^2 $TCID_{50}$ of CCHFV by the same routes resulted in identical disease signs, albeit with a slightly prolonged time to death (Figure 1*B*). The exception was intranasal inoculation which demonstrated decreased lethality at the low dose (17.6% lethality; Figure 1*B*). This model therefore recapitulates the broad susceptibility to routes of infection and differences in timing to disease onset, which are thought to occur in human cases [2, 35]. Although the model was originally characterized using the intraperitoneal route of inoculation [25, 26], to more closely simulate natural tick bite infection we used the subcutaneous route of inoculation for all subsequent experiments. The subcutaneous inoculation route is thought to better simulate tick bite–associated infections by targeting CCHFV to similar primary replication sites prior to virus spread. To establish the appropriate challenge dose, the LD_{50} by this route in $IFNAR^{-/-}$ mice was determined to be 0.05 $TCID_{50}$ (Figure 1*C*).

CCHFV Effectively Replicates and Causes Pathology in $IFNAR^{-/-}$ but Not WT Mice

To assess temporal changes in the virologic, pathologic, and immunologic parameters following CCHFV infection, a time course study was undertaken. Following subcutaneous inoculation with 200 LD_{50} (10 $TCID_{50}$) of CCHFV/animal, infectious CCHFV was recovered from organs of WT and $IFNAR^{-/-}$ mice as early as 24 hours after infection. Throughout the course of a 5-day infection, CCHFV titers did not significantly change in organs harvested from WT mice, with a constant low level ($\leq 1.1 \times 10^2 \pm 0.3 \times 10^2$ $TCID_{50}$/mg) of virus detected (Figure 2). In contrast, viral loads in $IFNAR^{-/-}$ mice increased over time, with peak titers documented in liver samples collected on day 4 after infection ($1.65 \times 10^4 \pm 0.52 \times 10^4$ $TCID_{50}$/mg; Figure 2). Viremia (as determined by the detection of infectious virus from whole blood samples) was only observed immediately preceding the time of death in $IFNAR^{-/-}$ mice. Quantitative RT-PCR results reflected the infectious titers from blood, and the negative RT-PCR results from earlier time points confirmed that CCHFV was not present at levels below the threshold of detection of the $TCID_{50}$ assay (Supplementary Figure 1). The appearance of disease signs prior to detectable viremia suggests a different mechanism of CCHFV dissemination in $IFNAR^{-/-}$ mice and is in contrast to the $STAT1^{-/-}$ mouse model, which reports viremia immediately following infection. However, the discrepancy is likely to arise from the inoculation method (subcutaneous vs intraperitoneal) and the inoculation dose (10 $TCID_{50}$ vs 100 plaque-forming units) [25]. While the period prior to appearance of viremia has not been evaluated in human CCHF, high viremia loads after onset of symptoms are often reported and are associated with severity of pathologic changes and with antigen staining and are an effective predictor of lethality [15–18, 20].

In our experiments, CCHFV antigen staining was not observed above background levels by IHC in any organs from infected WT mice (Supplementary Figure 2). In contrast, beginning at day 3 after infection, positively stained hepatocytes, Kupffer cells, and macrophages were apparent in the livers of $IFNAR^{-/-}$ mice, with the frequency and intensity of positively stained cells increasing until the terminal time point (day 4 after infection; Figure 3*A*). IHC analysis of $IFNAR^{-/-}$ lymphoid tissue (lymph node and spleen) demonstrated CCHFV antigen in cells that are morphologically consistent with macrophages. Additionally, there were rare immunopositive stellate cells that are morphologically consistent with dendritic cells (Figure 3*B* and 3*C*); once again, the frequency of antigen positive cells increased over time. Other tissues (ie, lung, kidney, and heart) displayed the same antigen-positive cells (endothelial cells and phagocytes) but at a lower frequency (data not shown). The histologic analysis correlates chronologically with virus detection.

Histologic analysis of organs from WT mice was unremarkable, with no discernible pathology identified at any time (Supplementary Figure 2). This was reflected by normal blood chemistry parameters (Figure 4*A* and 4*B*). Beginning at day 3 after infection, $IFNAR^{-/-}$ mice began to display significant pathologic changes in the liver, consisting of multifocal hepatocellular necrosis with infiltration of small-to-moderate numbers of viable and degenerate neutrophils (Figure 3*A*). The severity of liver damage increased, becoming coalescent at the terminal stage of disease. The degree of liver dysfunction was reflected by increased AST and ALT levels (Figure 4*A* and 4*B*). No other abnormal blood chemistry markers were noticed in CCHFV-infected $IFNAR^{-/-}$ mice. Mild-to-marked lymphocytolysis with loss of lymphocytes was noted in the cervical lymph nodes and splenic white pulp (Figure 3*B* and 3*C*). In addition, affected lymph nodes were frequently infiltrated by small-to-moderate numbers of viable neutrophils. At no time point were any histologic abnormalities observed in the lung, heart, kidney, or brain cross-sections from CCHFV-infected $IFNAR^{-/-}$ mice, despite the detection of infectious virus (Figure 2). The chronologic appearance of pathologic changes within the major target organs correlates with appearance of prominent viral antigen staining and viremia (compare Figure 2 with Figure 3), suggesting that high viral replication is responsible for the pathologic lesions observed as is thought to occur in humans [20]. The pathologic changes and high viral loads are thought to cause overstimulation of inflammatory cells, which are thought to play a leading role in the vascular abnormalities seen in CCHF [15]. While uncontrolled viral replication may be responsible for the pathologic changes in both human and $IFNAR^{-/-}$ CCHF, it is important

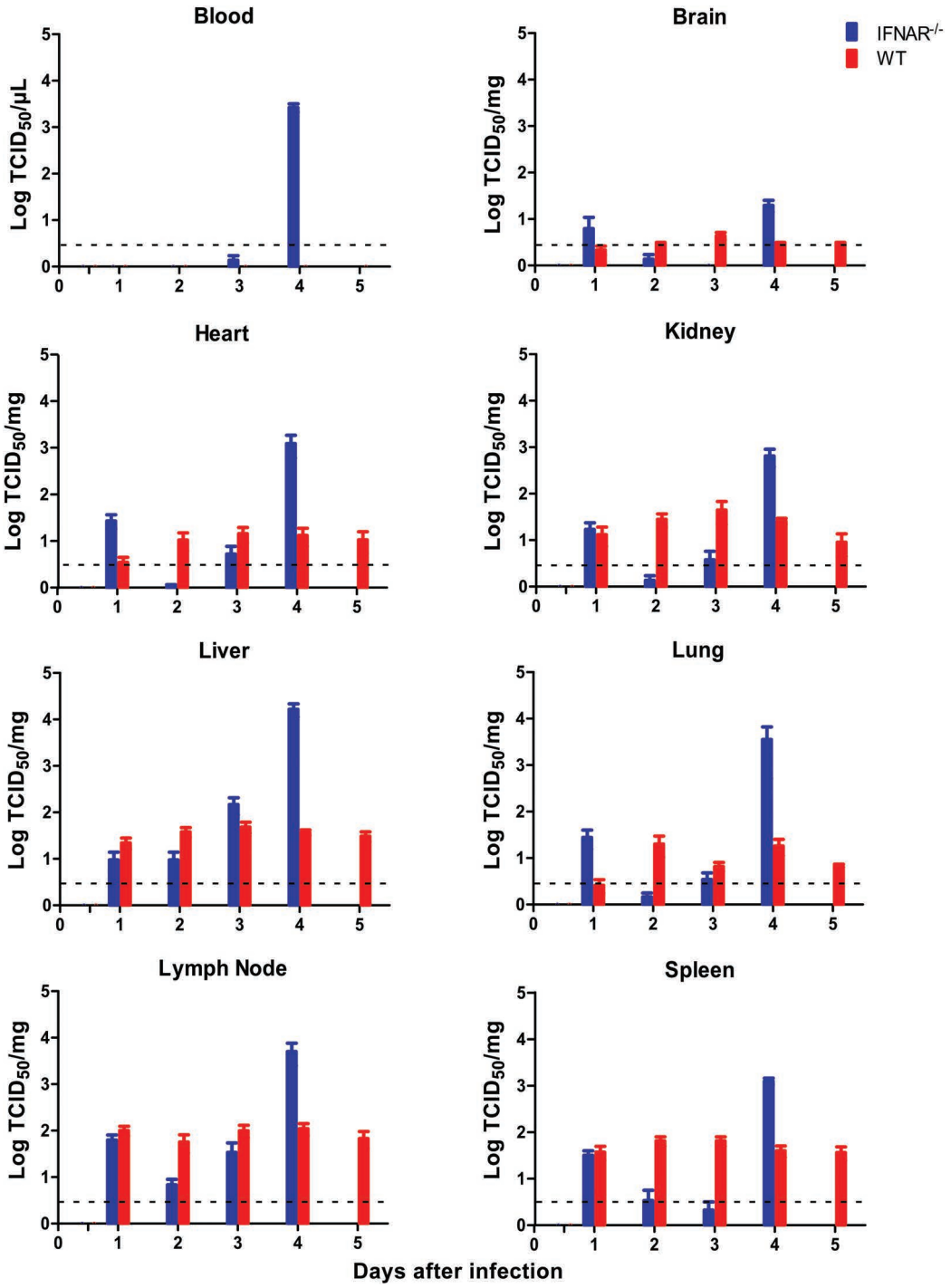

Figure 2. Viremia and organ viral titers of Crimean-Congo hemorrhagic fever virus (CCHFV) in wild-type and IFNAR$^{-/-}$ mice. Groups of 6 mice were inoculated with 200 50% lethal doses (10 median tissue culture infective doses [$TCID_{50}$]) of CCHFV by the subcutaneous route and sampled at indicated time points after infection. Viral titers were determined by standard $TCID_{50}$ assay and displayed as standard error about the mean. Dashed line represents the limit of detection of the $TCID_{50}$ assay (3.16 infectious particles per mg of tissue or µL of blood).

to note that CCHFV replication in humans requires the evasion of the type I IFN response. Therefore, the mechanisms of pathologic changes, while similar, are not necessarily identical between IFNAR$^{-/-}$ mice and humans.

CCHFV Infection Causes Thrombocytopenia and Coagulopathy in IFNAR$^{-/-}$ but Not WT Mice

Severe thrombocytopenia (up to a 90% reduction in the platelet level) is a hallmark and a predictor of fatality of severe

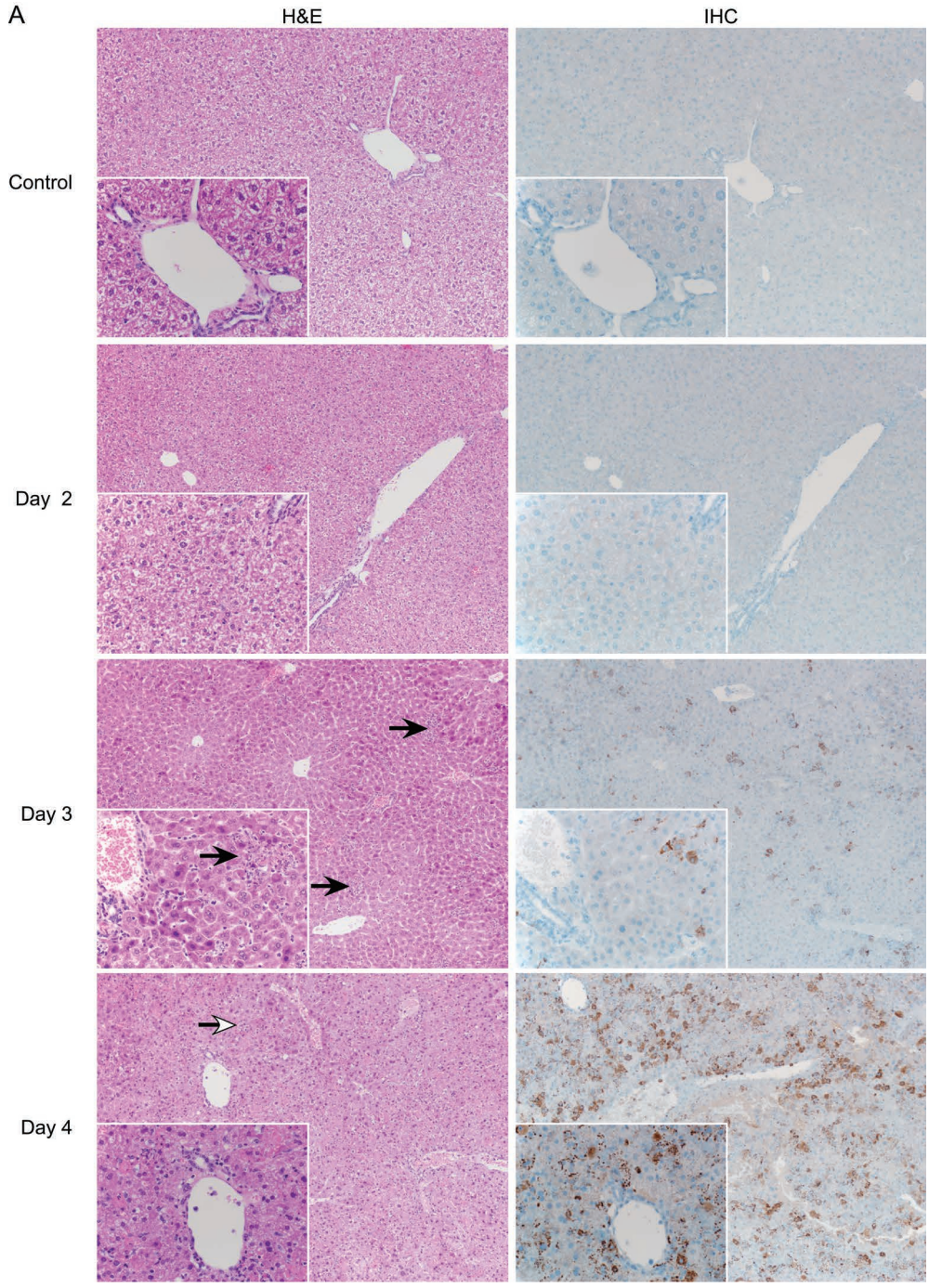

Figure 3. Histology (hematoxylin and eosin staining [H&E]) and immunohistochemistry (IHC) analysis of Crimean-Congo hemorrhagic fever virus (CCHFV) in IFNAR$^{-/-}$ mice. Groups of 6 mice were inoculated with 200 50% lethal doses (10 median tissue culture infective doses) by the subcutaneous route and sampled daily after infection. Tissues were stained with hematoxylin and eosin, H&E or a rabbit polyclonal serum directed against the CCHFV nucleoprotein (IHC). Histologic changes were first apparent on day 3 after infection. *A*, Liver displayed hepatocellular necrosis with infiltration of viable and degenerate neutrophils (solid arrows). The extent of pathologic changes increased over time, resulting in coalescing necrosis with loss of hepatic architecture beginning on day 4 after infection (open arrow).

CCHF in humans [1, 2, 25, 31–34, 36]. In contrast to CCHFV-infected WT mice, a significant decrease in platelet counts in infected IFNAR$^{-/-}$ mice was observed, beginning on day 3 after infection, that culminated in an approximately 90% decrease in counts by the terminal stage of infection (Figure 4*C*). The decrease in total platelets was accompanied by significant

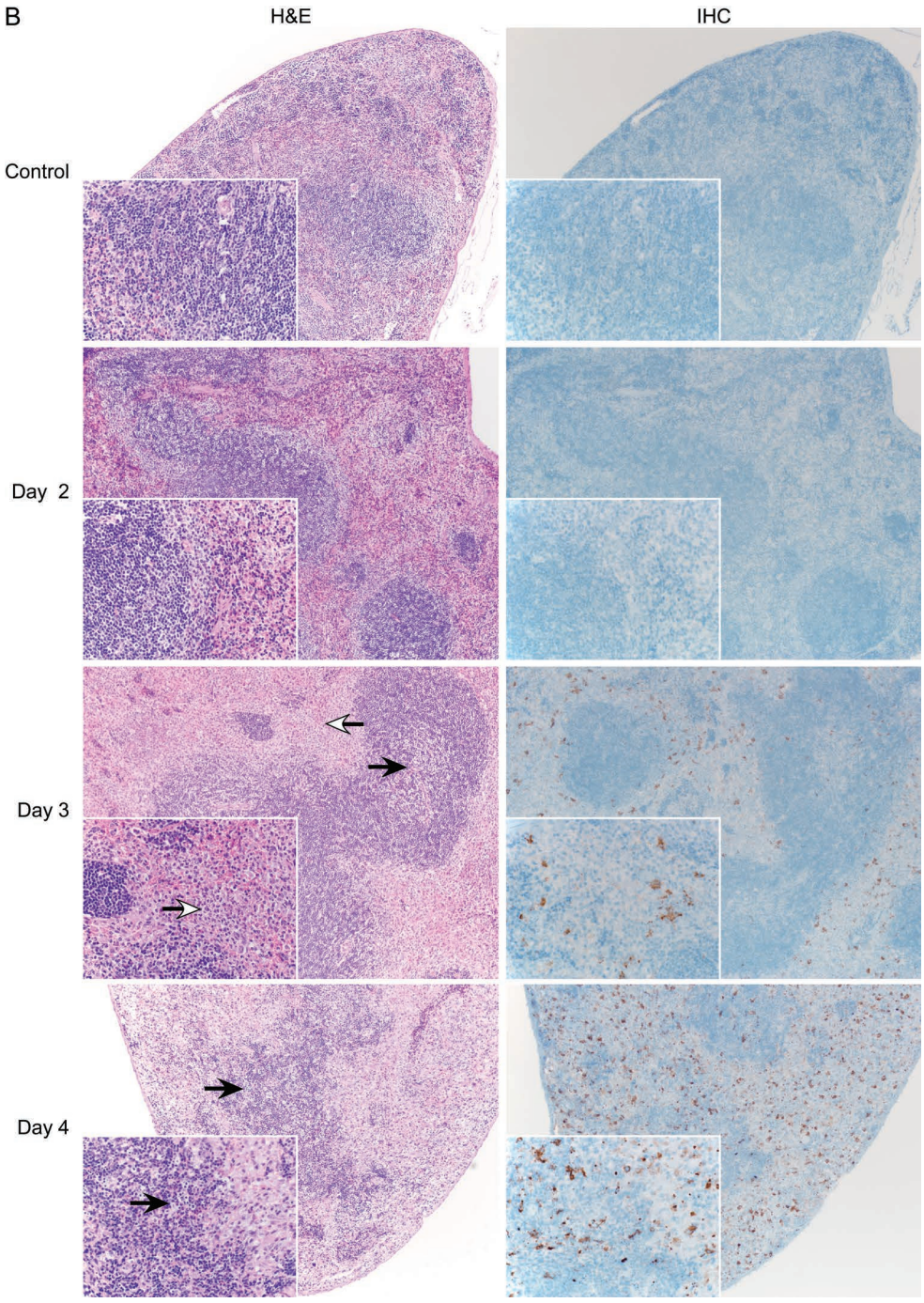

Figure 3 Continued. B, Spleen displayed diffuse lymphocytolysis with loss of lymphocytes from the white pulp (solid arrow) and diffuse infiltration of neutrophils (open arrows) by day 3 after infection. The extent of pathologic changes increased over time, with a marked loss of the white pulp by day 4 after infection.

increases in the mean platelet volume, suggesting platelet destruction as the likely mechanism of the decrease, as opposed to decreases in production (Figure 4*D*). Direct destruction of platelets is further supported by the accumulation of plasma fibrinogen levels over the disease course (Figure 4*E*) and by a lack of organ fibrin deposition, as demonstrated by hematoxylin and eosin and PTAH staining (Supplementary Figure 3), suggesting that the thrombocytopenia is not due to platelet activation, as reported for disseminated intravascular coagulopathy [37–39]. In addition, neither vascular leakage nor tissue

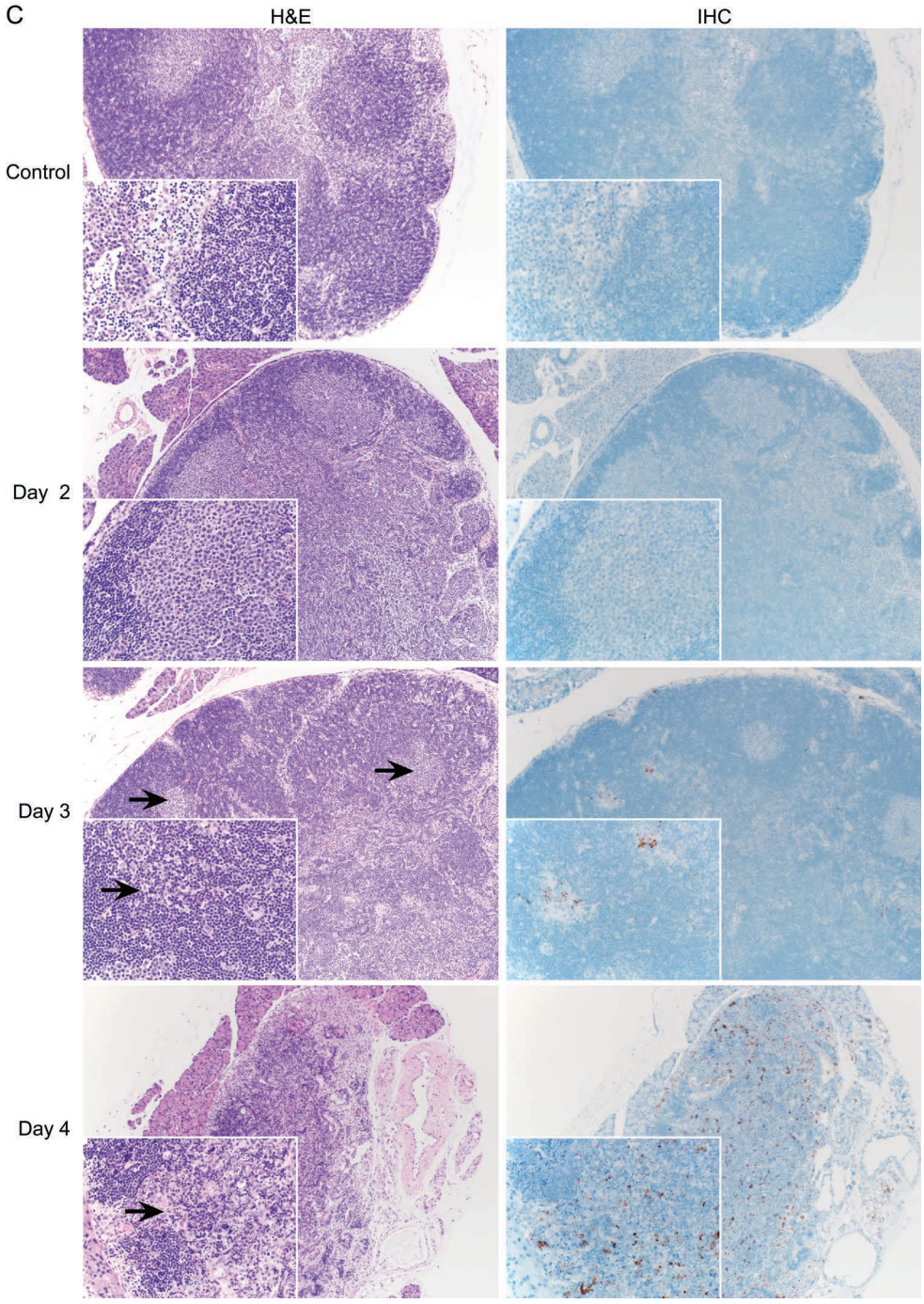

Figure 3 Continued. C, Lymph nodes display lymphocytolysis of follicular centers accompanying a loss of lymphocytes (solid arrows) by day 3 after infection. The severity of lymphocytolysis and loss of lymphocytes increased over time, resulting in loss of lymphoid architecture beginning at day 4 after infection. Note, shown here are representative samples of liver, spleen, and lymph nodes from mock-infected IFNAR$^{-/-}$ mice (control) and from CCHFV-infected IFNAR$^{-/-}$ mice on days 2, 3, and 4 after infection. Images are at a magnification of 10×, with 40× for the insets.

hemorrhages were detected by histologic analysis (data not shown). All other monitored parameters (hematologic, and blood chemistry) were static throughout the course of CCHFV infection in IFNAR$^{-/-}$ mice; CCHFV-infected WT mice did not show abnormalities in parameters tested here. The induced thrombocytopenia results in coagulopathy in IFNAR$^{-/-}$ mice but not WT mice, with a significantly increased activated partial thromboplastin time (Figure 4*F*). Prothrombin time

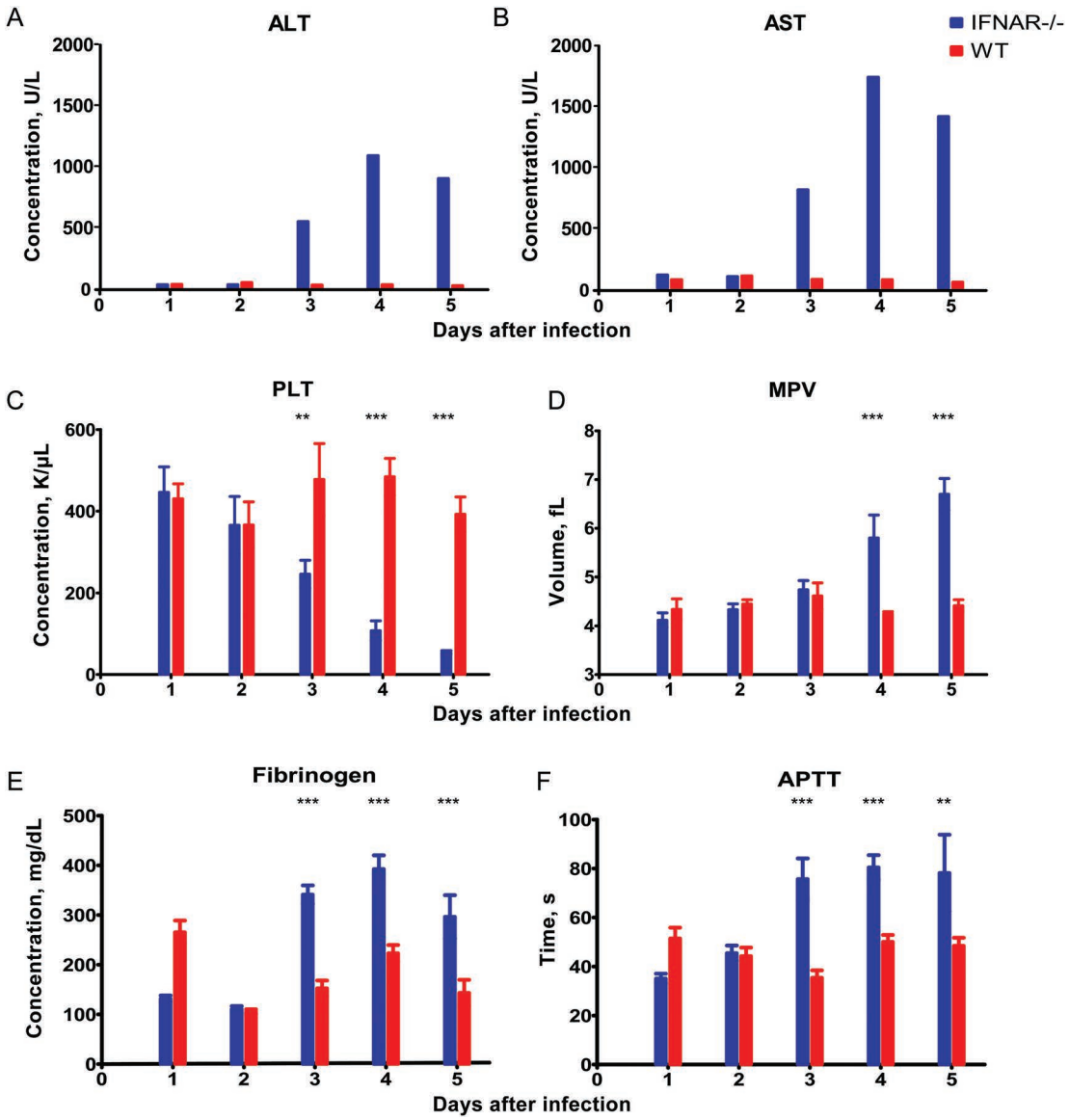

Figure 4. Abnormal hematologic, blood chemistry, and coagulation parameters following Crimean-Congo hemorrhagic fever virus (CCHFV) infection in wild-type (WT) and IFNAR$^{-/-}$ mice. A subset of mice were inoculated with 200 50% lethal doses (10 median tissue culture infective doses) by the subcutaneous route and exsanguinated at indicated time points (6 mice were used for hematologic analyses (except 3 IFNAR$^{-/-}$ mice on day 5 after infection), 7 mice were used for coagulation analysis (except 3 IFNAR$^{-/-}$ mice on day 5 after infection), and 1 pool (pools of 6 animal samples on days 1–4 after infection, a pool of 3 animal samples on day 5 after infection) was used for blood chemistry analysis. In contrast to CCHFV-infected WT mice, CCHFV-infected IFNAR$^{-/-}$ mice showed increased plasma alanine aminotransferase (ALT) levels (*A*), increased aspartate aminotransferase (AST) levels (*B*), decreased numbers of platelets (PLT; *C*), increased mean platelet volume (MPV; *D*), increased serum fibrinogen levels (*E*), and increased activated partial thromboplastin time (APTT; *F*). These data suggest that CCHFV infection of IFNAR$^{-/-}$ mice is associated with direct platelet destruction, rather than reduced platelet production. All data were analyzed by 1-way analysis of variance with the Dunnet posttest and are presented as standard error about the mean. ***$P < .001$ and **$P < .01$, compared with uninfected controls.

was unaffected throughout infection in both mouse species (data not shown). Together, the data suggest that IFNAR$^{-/-}$ mice faithfully reproduce major hallmarks of human disease and suggest that the thrombocytopenia is a result of the destruction of mature platelets.

CCHFV Infection Causes Strong Proinflammatory Immune Responses in IFNAR$^{-/-}$ but Not WT Mice

IFNAR$^{-/-}$ mice developed strong proinflammatory immune responses following CCHFV infection, as demonstrated by significant increases in G-CSF, IFN-γ, CXCL10, and CCL2

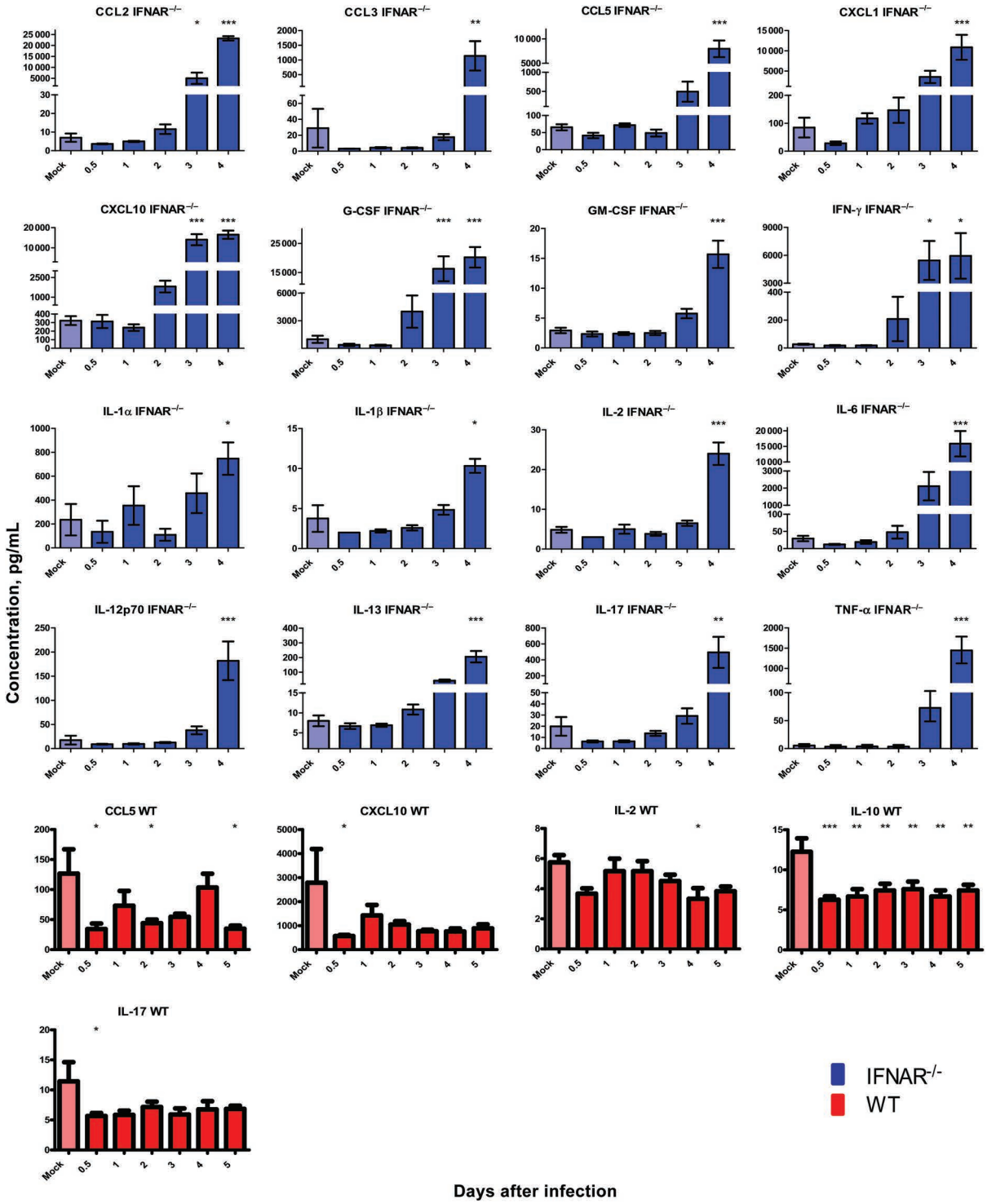

Figure 5. Cytokine and chemokine profiles following Crimean-Congo hemorrhagic fever virus (CCHFV) infection in wild-type (WT) and IFNAR$^{-/-}$ mice. Mice (n = 6) were inoculated with 200 50% lethal doses (10 median tissue culture infective doses) of CCHFV by the subcutaneous route and exsanguinated at indicated time points for evaluation of serum cytokine and chemokine levels. CCHFV-infected IFNAR$^{-/-}$ mice displayed marked increases in proinflammatory and chemoattractant molecules (blue graphs), whereas WT mice displayed selective reduction in certain proinflammatory and antiinflammatory molecules (red graphs). All data were analyzed by 1-way analysis of variance with the Dunnet posttest and are presented as standard error about the mean. *P < .05, **P < .01, and ***P < .001, compared with uninfected controls. Abbreviations: CCL2, monocyte chemotactic protein 1; CCL3, macrophage inflammatory protein 1α; CCL5, regulated upon activation, normal T-cell expressed, and secreted; CXCL1, chemokine (C-X-C motif) ligand 1 like; CXCL10, interferon-γ–induced protein 10; G-CSF, granulocyte colony stimulating factor; GM-CSF, granulocyte-macrophage colony stimulating factor; IFN-γ, interferon γ; IL-1α, interleukin 1α; IL-1β, interleukin 1β; IL-2, interleukin 2; IL-6, interleukin 6; IL-12p70, interleukin 12p70; IL-13, interleukin 13; IL-17, interleukin 17; TNF-α, tumor necrosis factor alpha.

concentrations, beginning on day 3 after infection, and in GM-CSF, IL-1α, IL-1β, IL-2, IL-6, IL-12p70, IL-13, IL-17, CXCL1, CCL3, CCL5, and TNF-α concentrations at the time of death/euthanasia (Figure 5). Proinflammatory cytokines and chemoattractant molecules observed in the sera of infected mice accumulated over the disease course, suggesting continuous overstimulation of the innate immune system by CCHFV replication. In contrast, WT mice displayed significantly decreased serum levels of IL-2, IL-10, IL-17, CCL5, and CXCL10 in response to CCHFV infection (Figure 5). The increases in serum proinflammatory cytokines in IFNAR$^{-/-}$ mice may represent an alternate, indirect mechanism of platelet destruction and is supported by the accumulation of fibrinogen levels observed in CCHFV-infected IFNAR$^{-/-}$ mice (Figure 4*E*).

CONCLUSIONS

IFNAR$^{-/-}$ mice are susceptible to multiple routes of CCHFV inoculation and develop fulminant lethal disease. Viral replication is readily detected in antigen-presenting and immune cells, which become activated and secrete high levels of chemoattractant and proinflammatory molecules. This activation, along with uncontrolled viral replication, results in pathologic changes and destruction of the liver and lymphoid organs and causes destruction of platelets, leading to coagulopathy, shock, and organ failure. Thus, the model closely recapitulates severe human CCHF in disease progression, pathophysiology, and pathology [1–3, 17–19, 40, 41]. Despite obvious limitations of the model due to the impaired IFN and immune response phenotype of the animals, IFNAR$^{-/-}$ mice currently represent the most appropriate animal disease model of CCHF. Therefore, this model should be used for future studies assessing the protective efficacy of countermeasures against CCHFV infections.

Supplementary Data

Supplementary materials are available at *The Journal of Infectious Diseases* online (http://jid.oxfordjournals.org/). Supplementary materials consist of data provided by the author that are published to benefit the reader. The posted materials are not copyedited. The contents of all supplementary data are the sole responsibility of the authors. Questions or messages regarding errors should be addressed to the author.

Notes

Acknowledgments. We are grateful to Dr Genhong Cheng (University of California, Los Angeles), for providing the foundation stock for establishing the IFNAR$^{-/-}$ mice breeding colony at Rocky Mountain Laboratories; staff at the Rocky Mountain Veterinary Branch (RMVB; Division of Intramural Research [DIR], National Institute of Allergy and Infectious Diseases [NIAID], National Institutes of Health [NIH]), especially Dr Rachel LaCasse and Kathleen Meuchel, for their assistance with the animal handling and animal procedures; Tina Thomas, Dan Long, and Rebecca Rosenke (RMVB, DIR, NIAID, NIH), for their help with preparation of pathology slides; Anita Mora (DIR, NIAID, NIH), for her help with graphics and art; and Tony Schountz (University of Northern Colorado, Greeley), for fruitful discussion regarding cytokine activation.

Financial support. This work was supported by the Division of Intramural Research, National Institute of Allergy and Infectious Diseases, National Institutes of Health.

Potential conflict of interest. All authors: No reported conflicts.

All authors have submitted the ICMJE Form for Disclosure of Potential Conflicts of Interest. Conflicts that the editors consider relevant to the content of the manuscript have been disclosed.

References

1. Whitehouse CA. Crimean-Congo hemorrhagic fever. Antiviral Res **2004**; 64:145–60.
2. Ergonul O. Crimean-Congo haemorrhagic fever. Lancet Infect Dis **2006**; 6:203–14.
3. Vorou R, Pierroutsakos IN, Maltezou HC. Crimean-Congo hemorrhagic fever. Curr Opin Infect Dis **2007**; 20:495–500.
4. Shepherd AJ, Leman PA, Swanepoel R. Viremia and antibody response of small African and laboratory animals to Crimean-Congo hemorrhagic fever virus infection. Am J Trop Med Hyg **1989**; 40:541–7.
5. Shepherd AJ, Swanepoel R, Cornel AJ, Mathee O. Experimental studies on the replication and transmission of Crimean-Congo hemorrhagic fever virus in some African tick species. Am J Trop Med Hyg **1989**; 40:326–31.
6. Swanepoel R, Leman PA, Burt FJ, et al. Experimental infection of ostriches with Crimean-Congo haemorrhagic fever virus. Epidemiol Infect **1998**; 121:427–32.
7. Zeller HG, Cornet JP, Camicas JL. Experimental transmission of Crimean-Congo hemorrhagic fever virus by west African wild ground-feeding birds to *Hyalomma marginatum rufipes* ticks. Am J Trop Med Hyg **1994**; 50:676–81.
8. Kaya A, Engin A, Guven AS, et al. Crimean-Congo hemorrhagic fever disease due to tick bite with very long incubation periods. Int J Infect Dis **2011**; 15:e449–52.
9. Cevik MA, Erbay A, Bodur H, et al. Clinical and laboratory features of Crimean-Congo hemorrhagic fever: predictors of fatality. Int J Infect Dis **2008**; 12:374–9.
10. Onguru P, Dagdas S, Bodur H, et al. Coagulopathy parameters in patients with Crimean-Congo hemorrhagic fever and its relation with mortality. J Clin Lab Anal **2010**; 24:163–6.
11. Weber F, Mirazimi A. Interferon and cytokine responses to Crimean Congo hemorrhagic fever virus; an emerging and neglected viral zoonosis. Cytokine Growth Factor Rev **2008**; 19:395–404.
12. Saksida A, Duh D, Wraber B, Dedushaj I, Ahmeti S, Avsic-Zupanc T. Interacting roles of immune mechanisms and viral load in the pathogenesis of Crimean-Congo hemorrhagic fever. Clin Vaccine Immunol **2010**; 17:1086–93.
13. Yesilyurt M, Gul S, Ozturk B, et al. The early prediction of fatality in Crimean Congo hemorrhagic fever patients. Saudi Med J **2011**; 32:742–3.
14. Yilmaz G, Koksal I, Topbas M, Yilmaz H, Aksoy F. The effectiveness of routine laboratory findings in determining disease severity in patients with Crimean-Congo hemorrhagic fever: severity prediction criteria. J Clin Virol **2010**; 47:361–5.
15. Ergonul O, Tuncbilek S, Baykam N, Celikbas A, Dokuzoguz B. Evaluation of serum levels of interleukin (IL)-6, IL-10, and tumor necrosis factor-alpha in patients with Crimean-Congo hemorrhagic fever. J Infect Dis **2006**; 193:941–4.
16. Papa A, Bino S, Velo E, Harxhi A, Kota M, Antoniadis A. Cytokine levels in Crimean-Congo hemorrhagic fever. J Clin Virol **2006**; 36:272–6.
17. Duh D, Saksida A, Petrovec M, et al. Viral load as predictor of Crimean-Congo hemorrhagic fever outcome. Emerg Infect Dis **2007**; 13:1769–72.

18. Wolfel R, Paweska JT, Petersen N, et al. Virus detection and monitoring of viral load in Crimean-Congo hemorrhagic fever virus patients. Emerg Infect Dis **2007**; 13:1097–100.
19. Papa A, Drosten C, Bino S, et al. Viral load and Crimean-Congo hemorrhagic fever. Emerg Infect Dis **2007**; 13:805–6.
20. Burt FJ, Swanepoel R, Shieh WJ, et al. Immunohistochemical and in situ localization of Crimean-Congo hemorrhagic fever (CCHF) virus in human tissues and implications for CCHF pathogenesis. Arch Pathol Lab Med **1997**; 121:839–46.
21. Peyrefitte CN, Perret M, Garcia S, et al. Differential activation profiles of Crimean-Congo hemorrhagic fever virus- and Dugbe virus-infected antigen-presenting cells. J Gen Virol **2010**; 91(Pt 1):189–98.
22. Kubar A, Haciomeroglu M, Ozkul A, et al. Prompt administration of Crimean-Congo hemorrhagic fever (CCHF) virus hyperimmunoglobulin in patients diagnosed with CCHF and viral load monitorization by reverse transcriptase-PCR. Jpn J Infect Dis **2011**; 64:439–43.
23. Schwarz TF, Nsanze H, Longson M, et al. Polymerase chain reaction for diagnosis and identification of distinct variants of Crimean-Congo hemorrhagic fever virus in the United Arab Emirates. Am J Trop Med Hyg **1996**; 55:190–6.
24. Tignor GH, Hanham CA. Ribavirin efficacy in an in vivo model of Crimean-Congo hemorrhagic fever virus (CCHF) infection. Antiviral Res **1993**; 22:309–25.
25. Bente DA, Alimonti JB, Shieh WJ, et al. Pathogenesis and immune response of Crimean-Congo hemorrhagic fever virus in a STAT-1 knockout mouse model. J Virol **2010**; 84:11089–100.
26. Bereczky S, Lindegren G, Karlberg H, Akerstrom S, Klingstrom J, Mirazimi A. Crimean-Congo hemorrhagic fever virus infection is lethal for adult type I interferon receptor-knockout mice. J Gen Virol **2010**; 91(Pt 6):1473–7.
27. Paragas J, Whitehouse CA, Endy TP, Bray M. A simple assay for determining antiviral activity against Crimean-Congo hemorrhagic fever virus. Antiviral Res **2004**; 62:21–5.
28. Reed LJ, Muench H. A simple method of estimating fifty per cent endpoints. Am J Epidemiol **1938**; 27:5.
29. Andersson I, Bladh L, Mousavi-Jazi M, et al. Human MxA protein inhibits the replication of Crimean-Congo hemorrhagic fever virus. J Virol **2004**; 78:4323–9.
30. Andersson I, Lundkvist A, Haller O, Mirazimi A. Type I interferon inhibits Crimean-Congo hemorrhagic fever virus in human target cells. J Med Virol **2006**; 78:216–22.
31. Ergonul O, Celikbas A, Baykam N, Eren S, Dokuzoguz B. Analysis of risk-factors among patients with Crimean-Congo haemorrhagic fever virus infection: severity criteria revisited. Clin Microbiol Infect **2006**; 12:551–4.
32. Ergonul O, Celikbas A, Dokuzoguz B, Eren S, Baykam N, Esener H. Characteristics of patients with Crimean-Congo hemorrhagic fever in a recent outbreak in Turkey and impact of oral ribavirin therapy. Clin Infect Dis **2004**; 39:284–7.
33. Ergonul O, Zeller H, Kilic S, et al. Zoonotic infections among veterinarians in Turkey: Crimean-Congo hemorrhagic fever and beyond. Int J Infect Dis **2006**; 10:465–9.
34. Tezer H, Sucakli IA, Sayli TR, et al. Crimean-Congo hemorrhagic fever in children. J Clin Virol **2010**; 48:184–6.
35. Nabeth P, Cheikh DO, Lo B, et al. Crimean-Congo hemorrhagic fever, Mauritania. Emerg Infect Dis **2004**; 10:2143–9.
36. Flick R, Whitehouse CA. Crimean-Congo hemorrhagic fever virus. Curr Mol Med **2005**; 5:753–60.
37. Levi M, de Jonge E, van der Poll T, ten Cate H. Disseminated intravascular coagulation. Thromb Haemost **1999**; 82:695–705.
38. ten Cate H, Timmerman JJ, Levi M. The pathophysiology of disseminated intravascular coagulation. Thromb Haemost **1999**; 82:713–7.
39. Levi M, Schultz M. Coagulopathy and platelet disorders in critically ill patients. Minerva Anestesiol **2010**; 76:851–9.
40. Cevik MA, Erbay A, Bodur H, et al. Viral load as a predictor of outcome in Crimean-Congo hemorrhagic fever. Clin Infect Dis **2007**; 45:e96–100.
41. Frias-Staheli N, Giannakopoulos NV, Kikkert M, et al. Ovarian tumor domain-containing viral proteases evade ubiquitin- and ISG15-dependent innate immune responses. Cell Host Microbe **2007**; 2: 404–16.